Volume : 2 | Issue : 8 | August 2013 • ISSN No 2277 - 8179

Research Paper

# Syntheses and Properties Characterizations of Titanium Oxide/ Cadmium Sulphide Nanocomposites by Chemical Bath Deposition Technique

Physics

**KEYWORDS :** $TiO_2$/CdS heterojunction, thin films, chemical bath deposition, bandgap.

| | |
|---|---|
| **B. A. Ezekoye** | Crystal Growth and Characterizations Laboratory, Department of Physics and Astronomy, University of Nigeria, Nsukka |
| **V. A. Ezekoye** | Department of Metallurgical and Materials Engineering, University of Nigeria |
| **F. I. Ezema** | Department of Metallurgical and Materials Engineering, University of Nigeria |
| **P.O. Offor** | Department of Metallurgical and Materials Engineering, University of Nigeria |
| **D. C. Obiegbunna** | Department of Metallurgical and Materials Engineering, University of Nigeria |

## ABSTRACT

*Heterojunction thin films of Titanium Oxide/Cadmium Sulphide (TiO2/CdS) were synthesized using chemical bath deposition (CBD) technique. The optical and structural characterizations showed that the samples have good transmittance in the visible and near infrared (NIR) region of the spectrum. The samples have very low reflectance within the visible region; hence will be good absorber of light. The absorption coefficient increases with increasing energy. The refractive index decreases with increasing energy, hence it has negative refractive index. The XRD studies revealed that samples became crystalline after annealing. The synthesized $TiO_2$/CdS thin films could serve as a window layer in the production of solar cells due to its wide energy band gap. Its optical properties such as low reflectance, high transmittance make it a good candidate for application in agriculture light and energy in the construction of poultry incubators. It could also find applications in transparent electronics.*

### 1.0 Introduction

Titanium dioxide (TiO2) thin films are of great interest to researchers due to their several applications as anti-reflection coatings for Si solar cells (Yeung & Lam, 1983). [1], semiconductor oxide gas sensors (Yimmizu & Egashira, 1999). [2], metal-oxide-semiconductor field effect transistor (MOSFET) gate electronics (Syzdio & Poirier, 1980). [3]. This is due to the characteristics of $TiO_2$ such as its high dielectric constant, high refractive index and good optical transmittance (Lee & Lai, 2002). [4]. Several methods has been used in synthesizing $TiO_2$ thin films such as physical vapour deposition (PVD), chemical vapour deposition (CVD), sol-gel and chemical bath depostion methods (Burns, Baldwin, Hatings, & Wikes, 1989; Lobl, Huppertz, & Mergel, 2000; Kamada, Kitagawa, Shibuya, & Hirao,1991; Alam & Cameron, 2005; Ea-Souni, Oja & Krunks, 2004; Chaure, Ray & Capan, 2005; Zhou, Hoffmann, Zhao, Bill & Aldinger, 2008).[5-11].

On the other hand, CdS is another interesting semiconductor binary compound belonging to the II-IV group of elements in the periodic table (Kotkata, Masoud, Mohammed, & Mahmoud, 2009) [12]. It has many optoelectronic applications in solar cells, light emitting diodes (LEDs), photodiodes, non-linear optical devices and heterogeneous photocatalysis (Kotkata et al, 2009) [12]. In this work $TiO_2$/CdS hetero junction thin films were synthesized using chemical bath deposition (CBD) technique. The as-grown samples annealed at different times and temperatures and characterized (optical and structural) for various technological applications.

### 2.0 Experimental Details

#### 2.1 Materials

The starting chemicals for the syntheses are gelatin, Sodium hydroxide (NaOH), Cadmium chloride ($CdC1_2$) Thiourea ($CS(NH_2)$) Titanium chloride ($TiCl_3$) Ammonia ($NH_3$), Hydrochloric acid (HCL), Distilled water ($H_2O$).

#### 2.2 Methods

Stock solutions of gelatin, sodium hydroxide (NaOH), cadmium chloride (CdCl), Thiourea, CS ($NH_2$), titanium chloride ($TiCl_2$), Ammonia ($NH_3$) hydrochloric acid (HCl) and distilled water were pr-prepared. Titanium dioxide was prepared by mixing appropriate volumes of titanium chloride ($TiCl_2$) and sodium hydroxide (NaOH), after which a clear glass slide was dipped into the solution and then suspended with synthetic foam. The setup was finally kept inside a thermostatic drying box at a temperature of 70 for a period of 4 to 5 hrs. The slides were then dried afterwards. The $TiO_2$ deposited films were again dipped into a prepared CdS solution and then left for a period of 2 minutes in thermostatic drying box of a temperature of 70°C. The now TiO2/CdS deposited glass slide is now removed and dried in air. The samples were annealed at various temperatures of 100°C for $C_{10}$, 200°C for $C_{20}$, 300°C for $C_{30}$, 400°C for $C_{40}$ and $C_{50}$ which was not annealed.

#### 2.2.1 Preparation of $TiO_2$ solution

2 ml of 1M NaOH solution was poured into a set of five 50 ml beakers and 50ml of $TiCl_2$ added to each set of 2ml of 1M NaOH solution. After 35 ml of gelatin solution was added into the set of five beakers already containing the initial solutions.

#### 2.2.2 Preparation of $TiO_2$ substrate

Five prepared microscopic glass slides were immersed into the $TiO_2$ solutions after it must have been stirred with a clean stirring rod. The immersed microscopic glass slides were suspended with synthetic foams so that there will be a homogeneous deposition of $TiO_2$ on substrates (glass slides) and also to protect the bath from dust and environmental contaminants. The setups were kept inside an electrothermal thermostatic drying box at a temperature of 70°C for a period of 4 to 5 hours. The slide containing the $TiO_2$ deposits were dried at room temperature.

#### 2.2.3 Preparation of $TiO_2$/CdS heterojunction

The $TiO_2$ deposited on microscopic glass slides were used as a substrate. These substrates were immersed into CdS solution and suspended with synthetic foams. The setups were then kept in an electrothermal thermostatic drying box, at a temperature of 70 °C. After about 2 minutes, the setups were brought out and the slides removed and dried, and a $TiO_2$ /CdS hetero junction thin films were formed.

#### 2.3 Mechanism of reaction

$Ti2 + + 4NaOH \longrightarrow [Ti(NaOH)4]2+$

$2NaOH + 2OH- \longrightarrow 2NaOH + NaCl2 + 2H2O$

$Ti2+ + 2O2- \longrightarrow TiO2 + O2$

$Cd2+ + NH3 \longrightarrow [Cd\ (NH3)4]2+$

$NH2CS+OH \longrightarrow SH- + H2O + H2CN2$

$SH+OH \longrightarrow S2+CdS$

**2.4 Heat Annealing of samples.**
These $TiO_2$/CdS hetero junction then films were then annealed at various temperatures and time intervals ranging from 400, 300, 200, 100°C for Samples $C_{10}$, $C_{20}$, $C_{30}$, and $C_{40}$ respectively. The $C_{50}$ Sample was as-grown.

**3.0 Results and Discussion**
**3.1 Optical Studies**
Optical properties of $TiO_2$/CdS heterojunction thin films were measured by UV–VIS spectroscopy. Fig. 1.c shows absorption spectra of $TiO_2$/CdS hetero junction. The absorption coefficient($\alpha$) is related to incident photons by the relation $\alpha h\nu = A(h\nu - E_g)^n$ (Kamada, Kitagawa, Shibuya, & Hirao,1991; Alam & Cameron, 2005; Ea-Souni, Oja & Krunks, 2004)[7, 8, 9], where $A$ is a constant and n is an index that characterizes the optical absorption process and is theoretically equal to 1/2, 2, 3/2 and 3 for direct allowed, indirect allowed, direct forbidden and indirect forbidden transitions, respectively. Since $TiO_2$/CdS hetero junction is a direct band gap semiconductor, the $(\alpha h\nu)^2$ versus the $h\nu$ diagram is depicted in Fig. 1.d. The tangent line on the curve shows the energy band gap of the thin $TiO_2$/CdS films varies from 1.60–2.40 eV.

The absorption coefficient ($\alpha$) was determined from the relation, $\alpha = \left(\frac{1}{d}\right)\ln\left(\frac{1}{T}\right)$, where d is the thickness of the film and T is the transmittance (Kamada, Kitagawa, Shibuya, & Hirao, 1991) [7] Fig.1(a) shows a plot of transmittance versus wavelength for $TiO_2$/CdS thin film samples $C_{10}$, $C_{20}$, $C_{30}$, $C_{40}$, and $C_{50}$

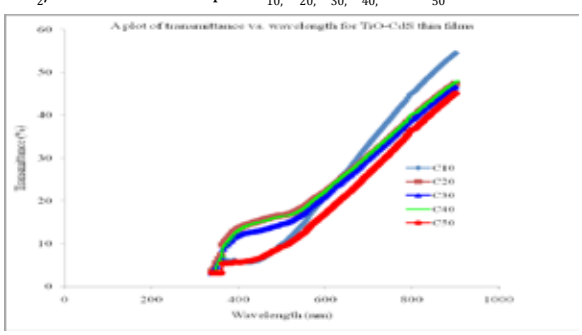


**Fig. 1a: Plot of transmittance versus wavelength for $TiO_2$/CdS Thin Film for Samples $C_{10}$, $C_{20}$, $C_{30}$, $C_{40}$, and $C_{50}$.**

From Fig.1a, there is an increase in transmittance as the wavelength increased. At the same wavelength of about 900 nm, the sample $C_{50}$ which is the unannealed sample, showed the least transmittance of 46% samples $C_{40}$, $C_{30}$ and $C_{10}$, had the same transmittance of about 48% this is a little above sample $C_{50}$ whereas sample $C_{20}$ had the best transmittance of 55%. It therefore shows that a $TiO_2$/CdS thin film annealed at a temperature of 200 °C will be most suitable for the use in the manufacture of optoelectronic devices.

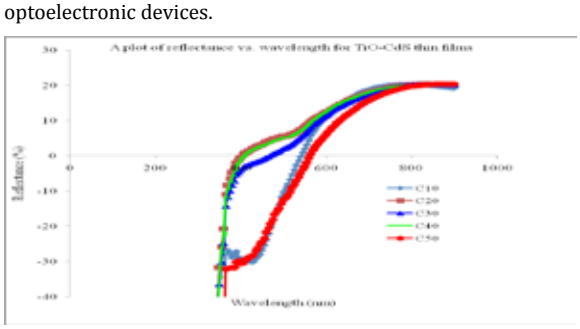


**Fig. 1b: Plot of reflectance versus wavelength for same samples**

Fig 1(b) shows also a plot of reflectance versus wavelength for same samples as above. From the graph, it is seen that samples $c_{20}$ and $c_{40}$ have negative reflectance of -40% at a wavelength of 400 nm. At this wavelength, the reflectance increased steadily until 0% where it starts again to increase. The reflectance becomes constant at 20% as the wavelength increases further. Samples $C_{30}$, $C_{10}$ and $C_{50}$ have negative reflectance of -40% at wavelength of about 500nm, 550 nm and 570 nm respectively. The negative reflectance of the samples shows that they are good absorbers and transmittances of visible light and infrared rays. Hence they are suitable for use in optoelectronics, solar energy cells, poultry house, *etc.*

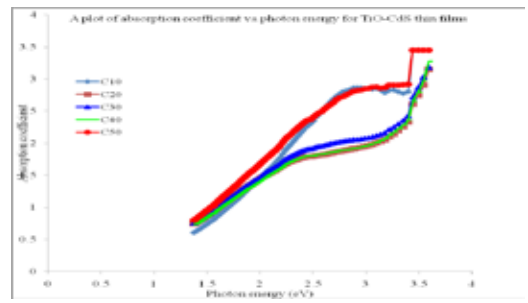


**Fig. 1c: Plot of Absorption Coefficient versus Photon Energy for $Ti0_2$/CdS**

**Thin Film Samples $C_{10}$, $C_{20}$, $C_{30}$, $C_{40}$ and $C_{50}$.**

Fig. 1c. on the other hand shows a plot of absorption coefficient versus photon energy for $Ti0_2$/CdS thin film samples $C_{10}$, $C_{20}$, $C_{30}$, $C_{40}$ and $C_{50}$.

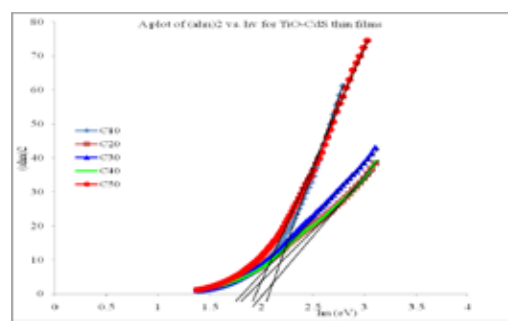


**Fig. 1d: Plot of ($\alpha$ h$\nu$)$^2$ (cm $^3$eV$^2$) versus Photon Energy h$\nu$ (eV) for $TiO_2$/CdS**
**Thin Films Samples for Samples $C_{10}$, $C_{20}$, $C_{30}$, $C_{40}$ and $C_{50}$.**

Fig. 1(d) shows a plot of ($\alpha$ h$\nu$)$^2$ (cm $^3$eV$^2$) versus h$\nu$(eV) for $TiO_2$/CdS thin films samples as above. From the graph, it is depicted that the photon energy starts from about 1.4 eV to increase towards the right. As it increases, the binding energy also increases. For samples $c_{10}$ and $c_{50}$, there is a sharp and exponential increase from 1.4ev. The same is obtainable for $C_{20}$,$C_{30}$,$C_{40}$. The only difference being that the later samples increased slowly. The direct bandgap for the materials ranges from 1.60 eV to 2.4 eV.

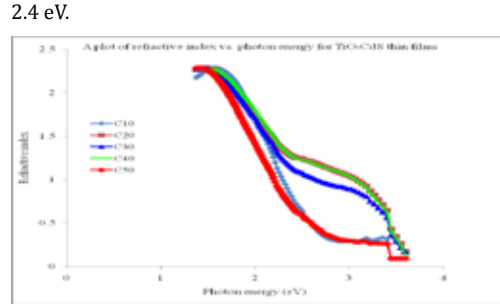


**Fig.1e: Plot of Refractive Index versus Photon Energy for $TiO_2$/CdS**
**Thin Films for Samples $C_{10}$, $C_{20}$, $C_{30}$, $C_{40}$ and $C_{50}$.**

Fig.1 (e) shows a plot of refractive index versus photon energy for $TiO_2$/CdS thin films $C_{10}$, $C_{20}$, $C_{30}$, $C_{40}$ and $C_{50}$. From the graph as the photon energy increases from 0 to 1.4 eV, there is no significant change in refractive index but as it increases further, a sharp decrease of refractive index from 2.25 to 1.25 is noticed samples $C_{40}$, $C_{30}$ and $C_{20}$ before recording a slow decrease and

then a further sharp decrease. For samples $C_{10}$ and $C_{50}$, there is a sharp decrease from 2.25 to 0.25 where it becomes constant. At 3.49 eV the refractive index had a sharp drop of refractive index and then finally becoming constant at 3.5 eV

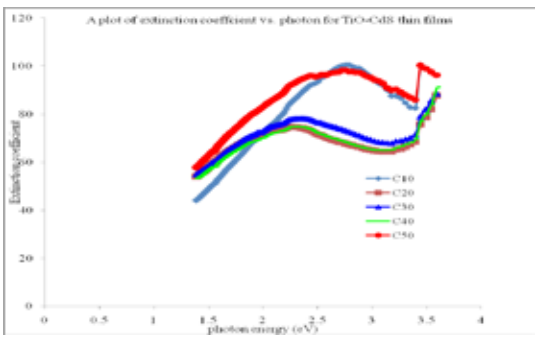


**Fig.1f: Plot of Extinction Coefficient versus Photon Energy for Samples for Samples $C_{10}$, $C_{20}$, $C_{30}$, $C_{40}$ and $C_{50}$.**

Fig.1 (f) shows a plot of extinction coefficient versus photon energy for samples as above from the graph, it is shown that $C_{20}$ had the hightest extinction coefficient of 100 at photon energy 2.75 eV followed by $C_{50}$ with the extinction coefficient of 98 at the same same photon energy 2.75 eV as $C_{20}$. Samples $C_{30}$ has the extinction coefficient 30 at photon energy of 2.25 eV samples $C_{20}$ while $C_{10}$ had similar extinction coefficient of 76 at photon energy 2.25 eV. It is observed that as the photon energy increased from 0 to 1.3 eV, there was no significance change in the extinction coefficient. But as it increased further from 1.3 eV, the extinction coefficient increased from 40 to 100 where it has its peak, before decreasing and eventually increasing.

### 3.2 Structural Studies

**Table 1: X-ray Diffraction Data**

| Sample | Peak / Theta | Grain Size/nm | FWHM/ Theta | Bandgap ($E_g$)/ eV |
|---|---|---|---|---|
| $C_{10}$ | 20, 70 | 38.5 | 4 | 1.60 – 2.40 |
| $C_{20}$ | 18, 91 | 25.4 | 6 | 1.60 – 2.40 |
| $C_{40}$ | 20, 820 | 38.5 | 4 | 1.60 – 2.40 |
| $C_{50}$ | 19, 550 | 25.6 | 6 | 1.60 – 2.40 |

Fig. 2 (a,b,c d) show the XRD spectra of the grown TiO/CdS thin films. The film structure was studied by X-ray diffraction (XRD) technique using the CuK $^{\alpha}$ a radiation ( $\lambda$ = 0.1790 nm) and the grain size or crystallite size D was obtained using the Debye Scherrer relation (Chaure, Ray & Capan, 2005) [10]:

$$D_{hkl} = \frac{K\lambda}{\beta \cos\theta},$$

where K=0.94, is the shape factor, $\lambda = 15408\text{Å}$, $\theta$ is the diffraction peak angle (Bragg angle) in degrees and $\beta$ is the full width at half maximum (FWHM) in radians, of the corresponding diffraction peak. Table 1 shows the various parameters of the grown films at 298, 473 and 673K. By increasing the annealing temperatures, the grain size of the crystallite was found to increase which is in agreement with Chaure, Ray & Capan, 2005). ref [10].

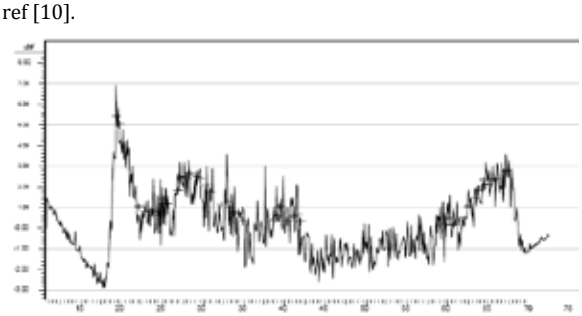

**Fig.2a: XRD Pattern for Sample C10**

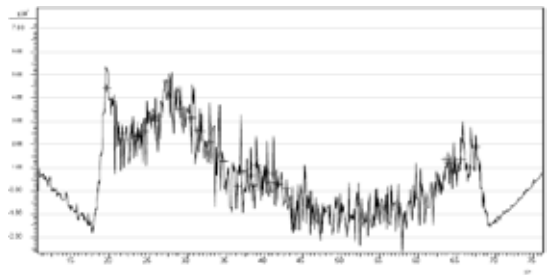

**Fig.2b: XRD Pattern for Sample C20**

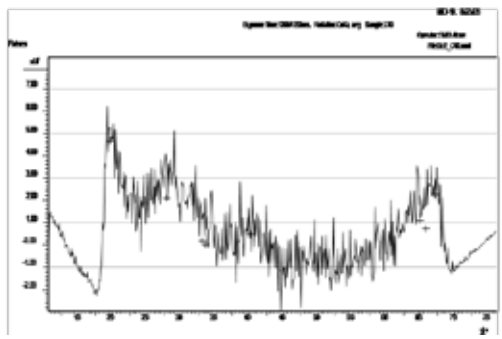

**Fig.2c: XRD Pattern for Sample C40**

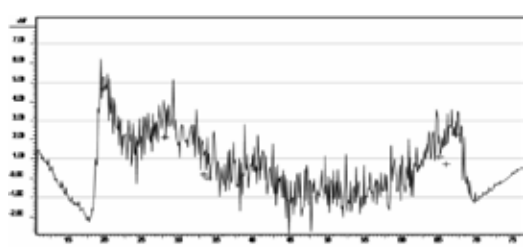

**Fig.2d: XRD Pattern for Sample C50**

The figures above show the XRD pattern recorded for $TiO_2$/CdS thin films $C_{10}$, $C_{20}$, $C_{40}$ and $C_{50}$. A close look at the figures revealed that Fig. 2 (a), 2(b), and 2(c) have close similarities and differ from 2(d). Fig.2 (a, b, c) all have very sharp peaks except 2(d). From the XRD pattern recorded, it can be seen that the samples' crystallinity increased with increase annealing temperature.

### 3.3 Compositional analysis of $TiO_2$/CdS Thin Film annealed at 400 °C

The Raman back scattering carried out on $TiO_2$/CdS thin film annealed at temperature 400 °C to determine its composition is as shown in Fig. 3 above. The RBS was carried out using beam of 2.20 MeV and FWHM of 12.0 keV as detector and the result is shown in Table 2.

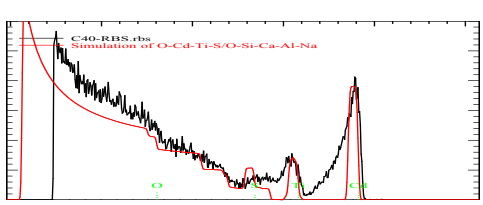


**Fig. 3: Rutherford Back Scattering Analysis**

**Table 2: Compositional Data and Thickness of the Films**

| No | Thick-ness/nm | Sub layers | Composition | | | | |
|---|---|---|---|---|---|---|---|
| 1 | 120.00 | auto | O-0.465 | Cd-0.121 | Ti-0.214 | S-0.200 | |
| 2 | 150.00 | auto | O-0.550 | Si-0.120 | Ca-0.050 | Al-0.050 | Na-0.230. |

Volume : 2 | Issue : 8 | August 2013 • ISSN No 2277 - 8179

### 3.3 Surface Morphology

Fig. 4.a. Sample C10

Fig. 4.b. Sample C20

Fig. 4c. Sample C30

Fig. 4d. Sample C40

The surface morphology of $TiO_2$/cds thin films $C_{10}$, $C_{20}$, $C_{30}$, $C_{40}$ and $C_{50}$ were studied at a magnification of x200 as shown in figures 4(a) 4(b), 4(c) 4(d) and 4(e). The as-grown films $C_{50}$ is amorphous while the heat treated films are polycrystalline ($C_{10}$, $C_{20}$, $C_{30}$, and $C_{40}$).

### 4.0 Conclusions

Thin films of $TiO_2$/CdS have been successfully deposited using adapted chemical bath method with bandgaps varying from 1.60 eV to 2.40 eV. From the optical, structural and compositional studies, we arrived at the following conclusions:

The samples have good transmittance in the visible and near infrared (NIR) region of the UV spectrum.

The samples have very low reflectance within the visible region, and hence will be good absorber of light.

The absorption coefficient increases with increasing energy.

The refractive index decreases with increasing energy and hence it has negative reflectivity

The samples became polycrystalline after annealing.

Compositional analysis revealed the existence of impurities such as oxygen, silicon, aluminum, calcium, and sodium in sample $C_{40}$.

Thin films of $TiO_2$/CdS are good candidates for very large applications in areas such as microelectronics, optoelectronics and photovoltaics. They can also serve as a window layer in the production of solar cells. Its optical properties such as low reflectance, high transmittance, makes it a good absorber of light and energy hence its application in agriculture for poultry incubators.

## REFERENCE

Alam, M.J., & Cameron, D. C. (2005). J. Sol-Gel Sci. Technol. 25, 137. | Burns, G. P., Baldwin, L. S., Hatings, M. P. & Wikes, J. G. (1989). J. Appl. Phys. 66, 2320. | Chaure, N. B., Ray, A.K. & Capan, R. (2005). Semicond. Sci. Technol. 20, 788. | Ea-Souni, M., Oja, I. & Krunks, M. (2004). J. Mater. Sci-Mater. Electron. 15, 341. | Kotkata, M. F., Masoud, A. E., Mohammed, M. B., & Mahmoud, E. A. (2009). Physica E. 41(8) 1457-1465. | Kamada, T., Kitagawa, M., Shibuya, M. & Hirao, T. (1991). Jpn. J. Appl. Phys. 30, 3594. | Lee, J. Y., Lai, B. C. in: H. S. Nalwa (Ed). (2002). Ferroelectric and Dielectric Film Materials, vol. 3, Academic Press, New York. | Lobl, P., Huppertz, M. & Mergel, D. (2000). Thin Solid Films, 406, 1032. | Syzdio, N. & Poirier, R. (1980). J. Appl. Phys. 51, 3310. | Yeung, K. S. & Lam, Y. W. (1983). Thin Solid Films, 109, 169. | Yimmizu, Y. & Egashira, M. (1999). MRS Bull. 24, 18. | Zhou, L., Hoffmann, R.C., Zhao, Z., Bill, J. & Aldinger, F. (2008). Thin Solid Films. 516, 7661-7666